

University of Nebraska - Lincoln

DigitalCommons@University of Nebraska - Lincoln

Faculty Publications, Department of Physics
and Astronomy

Research Papers in Physics and Astronomy

2012

Perpendicular magnetization in CoO (111) layers induced by exchange interaction with ferromagnetic Co and Ni₆₀Cu₄₀ nanoclusters

Damien Le Roy

University of Nebraska-Lincoln, damien.le-roy@grenoble.cnrs.fr

R. Morel

CEA, INAC, SP2M, 17 Rue des Martyrs, Grenoble F-38054, France

A. Brenac

CEA, INAC, SP2M, 17 Rue des Martyrs, Grenoble F-38054, France

S. Pouget

CEA, INAC, SP2M, 17 Rue des Martyrs, Grenoble F-38054, France

L. Notin

CEA, INAC, SP2M, 17 Rue des Martyrs, Grenoble F-38054, France

Follow this and additional works at: <https://digitalcommons.unl.edu/physicsfacpub>

 Part of the [Physics Commons](#)

Le Roy, Damien; Morel, R.; Brenac, A.; Pouget, S.; and Notin, L., "Perpendicular magnetization in CoO (111) layers induced by exchange interaction with ferromagnetic Co and Ni₆₀Cu₄₀ nanoclusters" (2012).

Faculty Publications, Department of Physics and Astronomy. 98.

<https://digitalcommons.unl.edu/physicsfacpub/98>

This Article is brought to you for free and open access by the Research Papers in Physics and Astronomy at DigitalCommons@University of Nebraska - Lincoln. It has been accepted for inclusion in Faculty Publications, Department of Physics and Astronomy by an authorized administrator of DigitalCommons@University of Nebraska - Lincoln.

Perpendicular magnetization in CoO (111) layers induced by exchange interaction with ferromagnetic Co and Ni₆₀Cu₄₀ nanoclusters

D. Le Roy,^{1,2,a)} R. Morel,³ A. Brenac,³ S. Pouget,³ and L. Notin³

¹Nebraska Center for Materials and Nanoscience, Lincoln, Nebraska 68588, USA

²University of Nebraska, Lincoln, Nebraska 68588, USA

³CEA, INAC, SP2M, 17 Rue des Martyrs, Grenoble F-38054, France

(Received 13 November 2011; accepted 8 March 2012; published online 16 April 2012)

The magnetization reversal of ferromagnetic nanoparticles coupled by exchange with a CoO (111) thin film has been studied. The interfacial exchange interaction triggers the appearance of an out-of-plane magnetization in the CoO (111) film. Co and Ni₆₀Cu₄₀ particles were chosen, as they present an order of magnitude difference in the saturation magnetization and Curie temperatures that surround the Néel temperature of CoO. In both cases, the exchange coupling leads to an increase of the coercive field, up to 200% in Co particles, and small exchange bias of 100 Oe when the external magnetic field is applied in the CoO (111) plane. When the field is applied along the CoO [111] direction, an unexpected net magnetization of the CoO (111) layer is revealed. Interestingly, it scales with the particles magnetization. The results are explained in terms of a large interfacial interaction and an induced canting of the CoO spins in the close region of the interface. The large value of the CoO magnetization indicates that the canting settles over an extended thickness of at least 3.7 nm and 1.2 nm in the cases of Co and Ni₆₀Cu₄₀ particles, respectively, which is consistent with a compensated antiferromagnetic spins surface.

© 2012 American Institute of Physics. [<http://dx.doi.org/10.1063/1.3702445>]

I. INTRODUCTION

The manifestation of the exchange interaction at the interface between a ferromagnet (FM) and an antiferromagnet (AFM) was first observed on partially oxidized Co particles more than fifty years ago.¹ In the commonly accepted picture, the interfacial exchange coupling results in the pinning of the FM spins. This phenomenon is widely used, notably in the hard drive disk technology,² and one can expect that it will play a major role in the emerging spintronic technology.³ Although the physics seems to be understood from a qualitative point of view,⁴ some questions remain regarding the microscopic mechanisms, mainly because of the experimental difficulties to (i) produce defects-free FM/AFM interfaces and (ii) determine the local spins configuration in a buried interface. Jiménez *et al.* have recently pointed out the key role that the interfacial defects play in the balance of the magnetic anisotropy at the interface.⁵ In FM nanoparticles (NPs), the anisotropy contribution induced by the exchange interaction with a surrounding AFM can be a way of beating the superparamagnetic limit.⁶ The commonly higher anisotropy of the AFM affects the FM spins reversal. However, in the case of core(FM)/shell(AFM) magnetic nanostructures, such as in Co/CoO NPs, the AFM shell presents reduced exchange and low anisotropy, owing to partial magnetic disorder.^{7,8} We have recently demonstrated that a large coupling can be obtained when FM NPs are deposited on an epitaxially grown AFM CoO (111) layer.⁹ The AFM spins configuration at the interface determines the pinning direction. As the FM/AFM is cooled down through the

Néel temperature (T_N), the magnetization of the FM is therefore determinant.¹⁰ In this report, both Co and Ni₆₀Cu₄₀ NPs are investigated. In the bulk state, these materials have Curie points (T_C) of 1400 K and 175 K,¹¹ respectively, which surrounds T_N of CoO (290 K). Besides, they present about one order of magnitude difference in both the T_C values and the saturation magnetization values, which are 1400 emu/cm³ for Co and about 100 emu/cm³ for Ni₆₀Cu₄₀, which could give information about the role played by the intrinsic FM exchange and the FM magnetic moment at the interface.

II. EXPERIMENTAL DETAILS

Co and Ni₆₀Cu₄₀ NPs were produced by sputtering and gas-condensation technique with a back pressure of 10⁻⁹ mbar.¹⁴ The NPs size was 4.4(4) nm, as monitored *in situ* by time of flight spectroscopy. Figure 1(a) shows typical NPs size distribution obtained in this study. The gas-aggregation conditions were tuned to obtain similar size distributions for both the materials. The equivalent thicknesses of Co and Ni₆₀Cu₄₀ NPs layers were 1 nm and 4 nm, respectively, in order to cover the CoO surface. These equivalent thicknesses correspond to percolated assemblies of NPs, which implies that interparticles' dipolar and exchange coupling are to be considered. For the Ni₆₀Cu₄₀ NPs synthesis, we used a sputtering target with the same stoichiometry. The composition of the formed Ni₆₀Cu₄₀ NPs was confirmed *ex situ* by energy-dispersive x ray spectroscopy with $\pm 2\%$ uncertainty. The NPs were deposited either on 20-nm Al₂O₃ thin films or on 20-nm CoO (111) layers obtained with the growth procedure described below. The NPs were protected from oxidation by a sputtered Al₂O_{3- δ} layer of 20 nm thick. In a previous report, we showed that only icosahedral Co NPs

^{a)}Author to whom correspondence should be addressed. Electronic mail: damien.le-roy@grenoble.cnrs.fr.

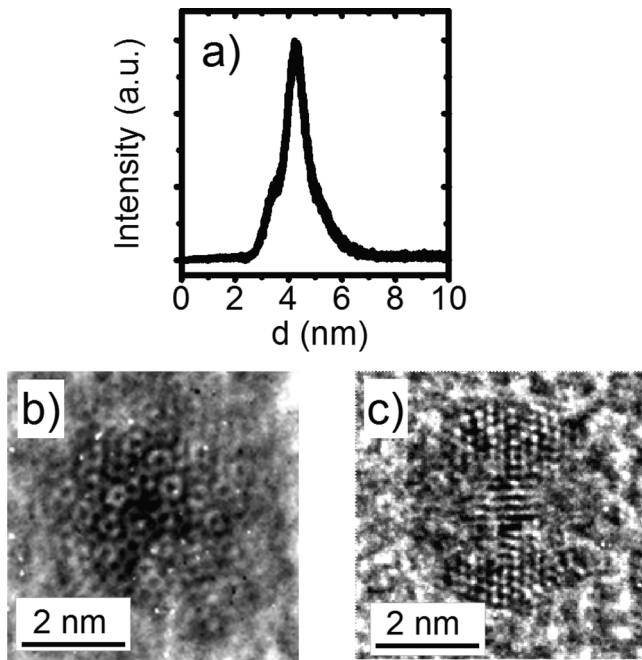


FIG. 1. (a) NPs size distribution measured *in situ* by time-of-flight spectrometry. (b) and (c) High resolution TEM images of a NiCu 4-nm $\text{Ni}_{60}\text{Cu}_{40}$ NP with the electron beam directed along its quinary axis (b) and its ternary axis (c).

were produced for sizes below 5 nm.¹⁴ Similar results were obtained for the $\text{Ni}_{60}\text{Cu}_{40}$ NPs. Figures 1(b) and 1(c) show two high resolution transmission electron microscopy (HRTEM) images of $\text{Ni}_{60}\text{Cu}_{40}$ NPs when the electron beam was directed along the icosahedron quinary axis (b) and binary axis (c). Note that the surface of the icosahedral NPs consists of (111) facets only and could be seen as a distorted assembly of twenty *fcc* tetrahedra. The lattice parameter determined by x ray diffraction (XRD) measurements was 0.359(3) nm, which corresponds to a composition of 70% Ni in the chemically disordered *fcc* structure. According to magnetic measurements, the saturation magnetization is close to the one observed early on in the disordered alloy in the bulk state. At this point, a chemical disordered structure is the most likely configuration.

The CoO (111) layers were deposited on an $\alpha\text{-Al}_2\text{O}_3$ (0001) substrate by reactive sputtering from a Co target in a mixed atmosphere Ar/O_2 at 200 °C, with a base pressure of 10^{-8} mbar. The epitaxial growth of CoO on $\alpha\text{-Al}_2\text{O}_3$ was demonstrated earlier by Gokemeijer *et al.*¹⁵ A detailed structural analysis of CoO layers was performed by means of a Seifert XRD 3003 PTS diffractometer using a Cu radiation and Ge(220) monochromators on incident and diffracted beams and HRTEM observations. In Fig. 2(b), one can see that the XRD pattern only shows CoO {*h*h*h*} reflections, *h* being an integer. The cross section HRTEM micrograph of Fig. 2(a) clearly reveals the stack of CoO (111) planes. Note that atomic force microscopy observations (not shown) showed a smooth interface with a 0.26(3) nm rms roughness. The presence of Laue fringes revealed around the CoO (111) Bragg-reflection peak (Fig. 2(c)) indicates sharp and smooth interfaces.

Magnetic measurements on NPs assemblies were performed by means of a Quantum Design superconducting

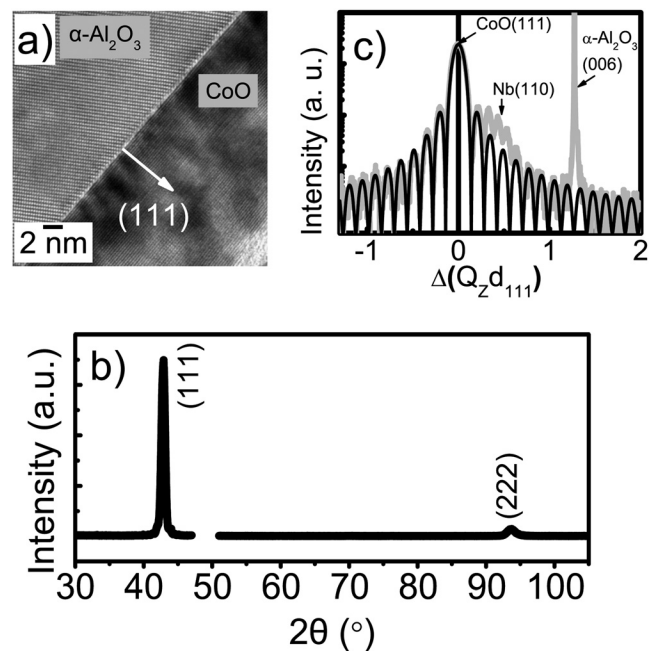


FIG. 2. (a) Cross-section TEM image of the CoO(111)/ $\alpha\text{-Al}_2\text{O}_3$ (0001) interface. (b) XRD pattern of Nb/ Al_2O_3 /NPs/CoO/ $\alpha\text{-Al}_2\text{O}_3$ (0001). The gap in the experimental data around $2\theta = 49^\circ$ corresponds to the position of the intense $\alpha\text{-Al}_2\text{O}_3$ (0006) peak. (c) Closer look of the XRD pattern around the CoO (111) Bragg-reflection peak.

quantum interference device (SQUID) magnetometer. The anisotropy constants K_1 and K_2 in CoO are, respectively, of $2.7 \times 10^8 \text{ erg/cm}^3$ and $2 \times 10^5 \text{ erg/cm}^3$.¹² Since the CoO layers are highly oriented in the polar [111] direction, both the in-plane (IP) and the out-of-plane (OOP) magnetizations were measured.

III. RESULTS AND DISCUSSION

A. In-plane magnetization measurements

Figure 3 shows the IP magnetization curves at 6 K for both $\text{Ni}_{60}\text{Cu}_{40}$ NPs and Co NPs either embedded into an Al_2O_3 matrix or deposited on CoO (111) layers and covered with a Al_2O_3 layer.

The saturation magnetization of the Co NPs was found to be the bulk one (1400 emu/cm^3), as for the $\text{Ni}_{60}\text{Cu}_{40}$ NPs (100 emu/cm^3), considering the mass uncertainty. It suggests that the CoO layer does not contribute to the magnetization, as expected for the highly ordered AFM layer. This also indicates that the NPs are not oxidized, since for the considered size, where more than 20% of the atoms occupy surface sites, a partial oxidation would lead to substantial reduction of the saturation magnetization. The magnetization curve along the CoO $[1\bar{1}0]$ azimuth was found to superimpose to the magnetization curve along the perpendicular azimuth CoO $[11\bar{2}]$.

The coercive field, H_C , increased from 0.5 kOe to 1.5 kOe with an exchange bias field, H_b , of 100 Oe for Co NPs, while in the case of $\text{Ni}_{60}\text{Cu}_{40}$ NPs, H_C increased from 100 Oe to 270 Oe with H_b of 55 Oe. The H_C increase was the most pronounced effect for both of the FM materials, as observed earlier by Givord in a system of Co NPs embedded into a CoO matrix with an interfacial perpendicular

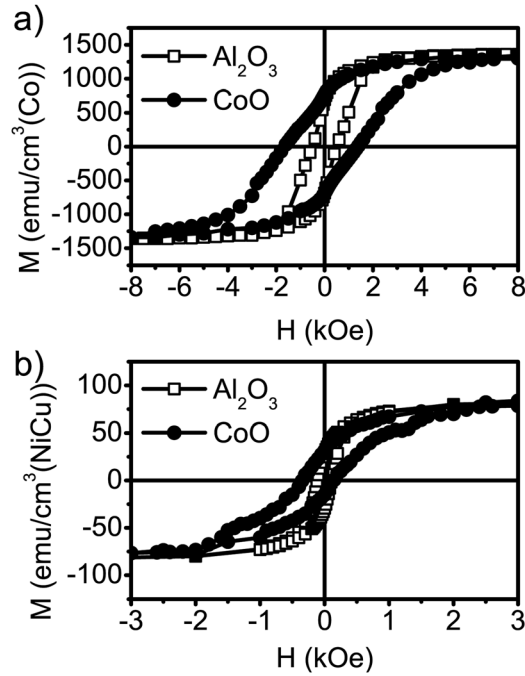


FIG. 3. IP magnetization curves at 6 K after field cooling under an external magnetic field of 30 kOe for (a) Co NPs and (b) $\text{Ni}_{60}\text{Cu}_{40}$ NPs. The magnetization is calculated using the volume of the FM.

coupling.¹³ This increase is generally associated to partial rotation of the AFM spins at the interface in a strong coupling configuration. On the other hand, the small H_b values denote a pinning that could be due to the pre-existing canting of the AFM spin moments at the interface.

These results suggest that the low value of K_2 results in a partial rotation of the spins in CoO during the FM magnetization reversal. One can then evaluate a volume V_{AFM} of the CoO layer in which the spins partially rotate using the increase of the coercive field ΔH_C ,

$$\Delta H_C = \frac{2K_{\text{AFM}}V_{\text{AFM}}}{M_{\text{FM}}V_{\text{FM}}}. \quad (1)$$

Considering the spherical-like morphology of the icosahedron, we consider an hemisphere-like volume for V_{AFM} with a radius R_{AFM} . It leads to $R_{\text{AFM}} = 3.2$ nm and $R_{\text{AFM}} = 0.8$ nm for the Co and $\text{Ni}_{60}\text{Cu}_{40}$ NPs, respectively. In the case we consider that the FM NPs coverage is large enough and the rotation of the AFM spins occurs within a critical and homogeneous thickness t_C in the AFM layer, we obtain t_C of 5.5 nm (for Co NPs) and 0.1 nm (for $\text{Ni}_{60}\text{Cu}_{40}$). Note that those values, relatively small, indicate that the rotation of AFM spins is restricted to an interface-close region and the magnetic ordering is not affected in the remaining AFM layer.

As mentioned before, exchange bias was observed in the $\text{Ni}_{60}\text{Cu}_{40}$ system, although the AFM ordering occurs while $\text{Ni}_{60}\text{Cu}_{40}$ is in the paramagnetic state, as expected if (i) the applied field during the cooling partially polarizes the PM spins of the NPs, which induces the ordering of the AFM, or (ii) the Zeeman energy terms acting on the AFM spin moments is sufficient to induce the ordering of the AFM.

B. Out-of-plane magnetization measurements

Figure 4 shows the IP and OOP magnetization curves at 6 K. Significantly smaller H_C was measured OOP in the case of Co NPs: 1500 Oe (IP) and 500 Oe (OOP). No such difference was observed in $\text{Ni}_{60}\text{Cu}_{40}$ NPs' magnetization with H_C of 300 Oe in the CoO [111] direction. Note that the overall magnetization of the NPs assembly is isotropic, since the NPs anisotropy axes are randomly oriented on the substrate surface. Thus, this anisotropy is related to the AFM for which the CoO [111] (OOP direction) constitutes a hard axis. Interestingly, the OOP-saturated magnetization exceeds the one of the sole assembly of Co and $\text{Ni}_{60}\text{Cu}_{40}$ NPs, while the IP saturated magnetization matches with the one of both bulk FM materials. An increase of the FM magnetic moment is unlikely, since it is, to our knowledge, neither proposed by calculation nor observed experimentally. In the opposite, the spins canting in the AFM layers has already been proven experimentally (by neutron scattering) and is supported by micromagnetic calculations.¹⁶ In this present work, this adding contribution to the OOP magnetization can only come from the CoO layer. It is worth to note here that no net magnetization has been observed for the sole CoO layer. This effect only occurred in the presence of the FM NPs, similarly to the spin-flop configuration observed by Borchers *et al.* in Co/CoO bilayers.¹⁷

The magnetic moment of the Co atoms in the CoO is $3.8 \mu\text{B}$. Our sample surface is 0.25 cm^2 . The [111] direction of CoO is a polar direction with alternating Co and O planes. The total magnetic moment hold by each Co plane corresponds to $8.3 \mu\text{emu}$. The large magnetic moment of Co rules

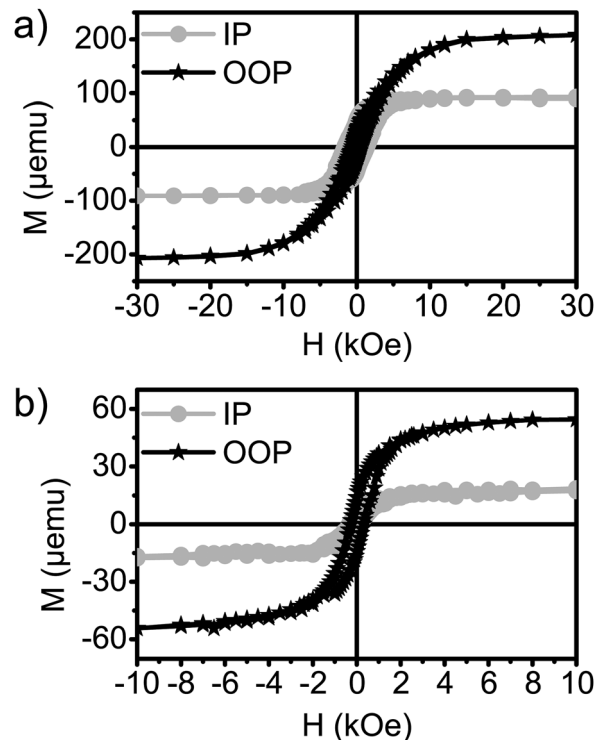


FIG. 4. IP and OOP magnetization curves at 6 K after field cooling under an external magnetic field of 30 kOe for (a) Co NPs and (b) $\text{Ni}_{60}\text{Cu}_{40}$ NPs.

out the sole contribution of uncompensated spins at the crystallites' boundary, which can be observed in other systems, such as Co/MnPt.¹⁸ Considering the same picture as proposed above for explaining the IP magnetization results, the OOP magnetization curves can be explained by a partial rotation of the AFM spins, with the difference that it results here in a net AFM magnetization contribution. This anisotropic CoO net magnetization could be related to the intrinsic anisotropy of CoO. Indeed, the high symmetry order of the spins structure in the CoO (111) planes is expected to facilitate the rotation of the AFM spins within the plane and keep an overall compensation.

It is worth to note that we did not observe any loop shift along the magnetization axis. In the absence of vertical shift, it is generally not possible to determine the sign of the interfacial exchange interaction from magnetization measurements. The first relevant indication of this adding contribution is the positive sign of the interfacial exchange interaction.

The net magnetic moment increase m_{CoO} is of $120 \mu\text{emu}$ in the case of Co and $36 \mu\text{emu}$ in the case of $\text{Ni}_{60}\text{Cu}_{40}$ NPs, fairly scaling with the FM magnetic moment. Note that, when observed, the contribution of the AFM magnetic moments to the magnetization is marginal.¹⁹ The particularity of our system could be the single domain feature of the FM nanoclusters that can preclude the generally admitted picture of a domain wall parallel to the interface in the FM.

The following discussion is focused on the spins configuration at the interface. In bulk CoO, CoO (111) planes are uncompensated spins planes. The spins are pointing in the $[\bar{1}\bar{1}7]$ that is 23.8° off from the (111) plane. Considering a layer orientation $[11\bar{1}]$, the spins orientation is at 55.5° from the normal to the film plane.

First consider a limit case in which the AFM spins are collinear to the FM spins within a distance t_c from the FM/AFM interface and aligned on their anisotropy axis in the remaining CoO volume. This configuration is energetically favorable for exchange interaction matter, but neglects the cost in anisotropy energy. Therefore, it can be used to estimate an inferior limit of t_c . m_{CoO} corresponds to the total magnetic moment of 15 atomic Co planes in CoO in the case of Co NPs and 5 atomic Co planes in CoO in the case of $\text{Ni}_{60}\text{Cu}_{40}$ NPs that correspond to $t_c \approx 3.7 \text{ nm}$ and $t_c \approx 1.2 \text{ nm}$, respectively. The exchange is a short-range interaction and so is limited to the nearest neighbors. Thus, the compensation of the AFM magnetization is expected to recover within a few atomic layers from the interface if we consider the case of a fully uncompensated AFM surface. This large value of m_{CoO} can only be explained by compensated Co spins planes along the CoO [111] growth direction. Note that three of the equivalent $\langle 111 \rangle$ directions in CoO would lead to compensated spins surface. A schematic diagram of a possible spins configuration is displayed in Fig. 5. One can distinguish two AFM regions: at a distance $t > t_c$ from the interface, the AFM spins are aligned on their anisotropy axis, while for $t < t_c$, the AFM spins are tilted. The competing anisotropy and exchange energies result in a gradual increase of the canting toward the interface. As a result, a net magnetic moment in the CoO layer appears along the applied field direction, i.e., CoO [111].

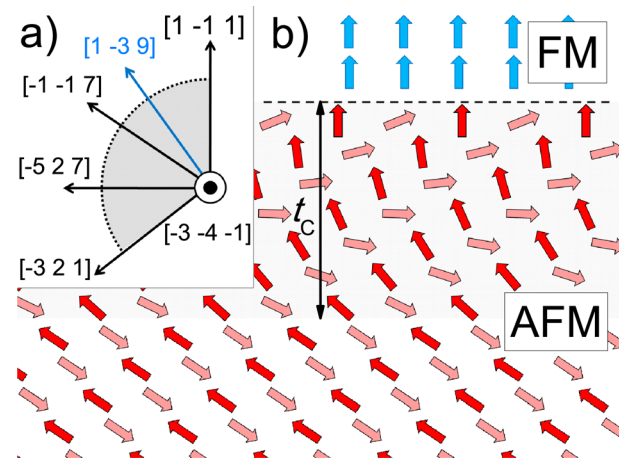


FIG. 5. Schematic picture of the spins configuration at the FM/AFM interface, projected in CoO $(\bar{3}\bar{4}\bar{1})$. The frame of reference (a) shows the relevant directions within the representation plane that contains the growth direction CoO $[1\bar{1}1]$ and the direction of the spins CoO $[\bar{1}\bar{1}7]$, considering that the magnetic order in the volume of the CoO layer is the one of the bulk. The CoO $[1\bar{3}9]$ is the direction of the projected CoO $[1\bar{1}1]$ direction in the CoO $(\bar{3}\bar{4}\bar{1})$ plane. In (b), the arrows represent the spins moments' orientations on both sides of the FM/AFM interface, with the suggested interfacial canting discussed here. Note that only Co atoms are represented in the CoO side.

IV. CONCLUSION

The interfacial interaction between FM NPs of Co and $\text{Ni}_{60}\text{Cu}_{40}$ with an underneath layer of CoO (111) has been investigated. Our results show that the exchange interaction leads to partial rotation of the AFM spins close enough to the FM/AFM interface. The in-plane coercivity increases up to 200% for Co NPs. The small value of K_2 allows this partial rotation to occur, and a global AFM spins compensation is conserved. However, when the external magnetic field is applied out of plane, the interfacial coupling triggers the appearance of a net magnetization in the CoO layer. This result reveals how the exchange coupling settles in this system; in particular: (i) the exchange interaction sign at the interface is positive and (ii) the AFM spins canting occurs in an extended volume of the CoO layer. In the case of Co NPs, an inferior limit of this volume was estimated to 65%, which seems to be consistent only with a compensated spins configuration at the surface of the CoO.

¹W. H. Meiklejohn and C. P. Bean, *Phys. Rev.* **105**, 3 (1957).

²B. Dieny, V. S. Speriosu, S. S. Parkin *et al.*, *Phys. Rev. B* **43**, 1297 (1991).

³P. Borisov, A. Hochstrat, X. Chen *et al.*, *Phys. Rev. Lett.* **94**, 117203 (2005).

⁴J. Nogues, J. Sort, V. Langlais *et al.*, *Phys. Rep.* **422**, 65 (2005).

⁵E. Jiménez, J. Camarero, J. Sort, J. Nogués *et al.*, *Phys. Rev. B* **80**, 014415 (2009).

⁶V. Skumryev, S. Stoyanov, Y. Zhang *et al.*, *Nature* **423**, 850 (2003).

⁷A. N. Dobrynin, D. N. Levlev, K. Temst, and P. Lievens, *Appl. Phys. Lett.* **87**, 012501 (2005).

⁸C. Portemont, R. Morel, W. Wernsdorfer *et al.*, *Phys. Rev. B* **78**, 144415 (2008).

⁹D. Le Roy, R. Morel, S. Pouget *et al.*, *Phys. Rev. Lett.* **107**, 057204 (2011).

¹⁰M. G. Blamire, M. Ali, C.-W. Leung *et al.*, *Phys. Rev. Lett.* **98**, 217202 (2007).

¹¹A. J. P. Meyer and C. Wolff, *C. R. Acad. Sci.* **246**, 576 (1958).

¹²C. Mocuta, Ph.D. dissertation, Université Joseph Fourier, 2003.

¹³D. Givord, *J. Magn. Magn. Mater.* **294**, 111 (2005).

- ¹⁴R. Morel, A. Brenac, P. Bayle-Guillemaud *et al.*, *Eur. Phys. J. D* **24**, 287 (2003).
- ¹⁵N. J. Gokemeijer, R. L. Penn, D. R. Veblen, and L. C. Chien, *Phys. Rev. B* **63**, 174422 (2001).
- ¹⁶A. Baruth, D. J. Keavney, J. D. Burton *et al.*, *Phys. Rev. B* **74**, 054419 (2006).
- ¹⁷J. A. Borchers, Y. Ijiri, S.-H. Lee *et al.*, *J. Appl. Phys.* **83**, 7219 (1998).
- ¹⁸R. Morel, C. Portemont, A. Brenac, and L. Notin, *Phys. Rev. Lett.* **97**, 127203 (2007).
- ¹⁹H. Ohldag, A. Scholl, F. Nolting *et al.*, *Phys. Rev. Lett.* **91**, 017203 (2003).